

NONLINEAR ANALYSIS OF A REINFORCED CONCRETE MOCK-UP UNDER SEISMIC LOADING



B. Richard¹

(1) CEA, DEN, DM2S, SEMT, Laboratoire d'Etudes Mécanique et Sismique, F-91191 Gif-sur-Yvette, France

F. Ragueneau²

(2) ENS/LMT Cachan Université Paris 6/CNRS/PRES UniverSud, 61 Avenue du Président Wilson, 94230 Cachan, France

SUMMARY:

In 2006, a joint research project aiming at studying the seismic structural behaviour of irregular in plan reinforced concrete structures has been started by CEA and EDF. The aim of this project was (i) to compare and validate approaches used for quantifying the dynamic responses evaluation of RC structures subjected to earthquakes and exhibiting 3D nonlinear effects, (ii) to evaluate loads induced to internal equipment, (iii) to quantify margins in design methodologies and (iv) to carry out realistic methods to quantify variability in order to produce fragility curves. In this paper, a numerical analysis of the reinforced concrete mock-up using a new constitutive law for concrete is presented. In particular, the numerical results show that the constitutive law can be used for accurate and fine analysis of complex structures subjected to seismic loadings.

Keywords: Concrete; Constitutive law; Isotropic damage mechanics; SMART 2008

1. INTRODUCTION

Last decades have witnessed a growing interest of the international scientific community for assessing the mechanical behavior of reinforced concrete structures subjected to earthquakes. Especially, important financial supports have been deployed in the case of nuclear based design structures. In interactions with the experimental programs that have been carried out last years, numerical benchmarks were also considered to evaluate the efficiency and the reliability of constitutive laws used for describing the nonlinear behavior of concrete. Indeed, concrete is a quasi-brittle material exhibiting asymmetric response in tension/compression due to cracking, a sensitivity to the hydrostatic pressure in the case of biaxial compression, hysteretic effects when unloading, permanent strains in tension and in compression and the unilateral effect characterizing the crack closing. The accuracy of the overall structural model is mainly dependent on the accuracy and the identification of local constitutive laws. Recently, a new constitutive law for concrete has been proposed, accounting for refine phenomena such as those aforementioned. In this study, one investigates the possibilities offered by this new constitutive law to deal with the dynamic behavior of a reinforced concrete structure designed for nuclear applications subjected to seismic loadings. Quantitative comparisons between experimental results and experimental data have been realized leading to some concluding remarks on the relevancy of the proposed constitutive law. This paper is outlined as follows. First, the experimental campaign under study is presented in a short way. Especially, the seismic inputs as well as the experimental outputs considered in this analysis are shown. Second, the numerical constitutive law is discussed. A specific attention to the material parameters identifications has been paid. The structural model is described. Among the main features of the proposed model, one can highlight the fact that the shaking table/structure interaction has been taken into account by considering a simplified model of the experimental device. Last, the numerical results are compared to the experimental ones allowing some useful comparisons on the efficiency of the concrete constitutive law used in this study.

2. EXPERIMENTAL CAMPAIGN SMART 2008

2.1. Reinforced concrete mock-up

The mock-up is representative of a typical nuclear building (half part of an electrical building) at a scale of 1/4. The SMART-2008 mock-up was designed by IOSIS Industries. It is composed of three walls forming a U shape, as shown on Figure 1. Two of those walls have openings as shown in Figure 2. The dimensions of the different structural elements are given in Table 1.

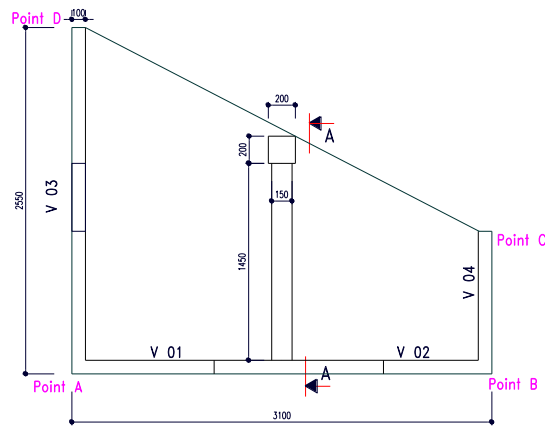


Figure 1. Plan view of SMART2008 mock-up.

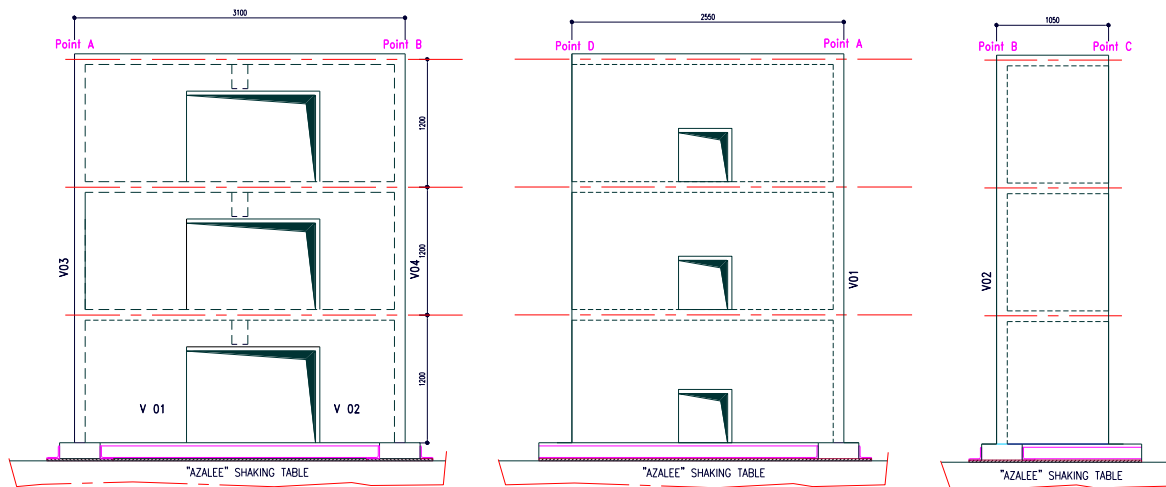


Figure 2. Elevation views of SMART 2008 mock-up.

Table 1. Dimensions of the main structural components

Structural component	Length (m)	Thickness (m)	Height (m)
Wall (#V01 + #V02)	3.10	0.10	3.65
Wall #V03	2.55	0.10	3.65
Wall #V04	1.05	0.10	3.65
Beam	1.45	0.15	0.325
Column	3.80	0.20	0.20

The wall's foundations are made of a continuous reinforced concrete footing. The footing is 38 cm wide, 15 cm high and lies on a steel plate (62 cm large and 2 cm thick). The reinforced concrete column is anchored on a 62cm x 62cm steel plate. The mock-up is bolted on the AZALEE shaking table through the base steel plates of the foundation and the column with 40 thread stalks, diameter 36

mm. Additional “L” steel pieces (120 mm x 120 mm x 12 mm) have been added on steel plates before tightening the nuts in order to rigidify the foundation system. In order to have a uniform contact between the steel plates and the shaking table, a grout without contraction was put under the steel plates before tightening the nuts. It was not necessary to put grout under the column base plate. All the nuts were tightened after the drying of the grout. The mock-up was not moved from this time up to the end of the seismic tests.

2.2. Material properties

Both concrete and steel reinforcing bars have been subjected to design mechanical testing in order to qualify their respective behaviour. The results are presented in Tables 2 and 3 for concrete and steel respectively.

Table 2. Material parameters for concrete

Structural component	Compressive strength (MPa)	Tensile strength (MPa)	Young's modulus (GPa)
Foundation	35	2.90	31.5
Walls and column - 1st level	32.5	3.05	30.5
Slab and beam - 1st level	28	2.65	29
Walls and column - 2nd level	29.5	2.60	26.5
Slab and beam - 2nd level	36	2.90	31.5
Walls and column - 3rd level	30	2.65	33.5
Slab and beam- 3rd level	32	2.55	29.5

Table 3. Material parameters for steel

Diameter (mm)	Young's modulus (GPa)	Yielding stress (MPa)
10	205	605
8	180	538
6	180	537
4	184	522
3	205	753

2.3. Additional masses

The average concrete density, based on the weight of the cylindrical concrete samples, is estimated to about 2372 kg.m^{-3} , and the one of the steel reinforcement at about 7.85 kg.m^{-3} . The average density of the reinforced concrete of the structure can be approximated to about 2460 kg.m^{-3} which is coherent with the density conventional values (between 2400 kg.m^{-3} and 2500 kg.m^{-3}). The self-weight of the mock-up was measured and is equal to 10.44 t. In order to respect the similitude law selected, the mock-up must be loaded with an additional mass equal to three times the dead load of the mock-up, i.e. around 31.5 t. Therefore, the total weight of the mock-up should reach a value of 42 Tons. Steel and lead blocks were used as additional masses, as they were available at the laboratory. Only few blocks were specifically delivered in order to complete the loading. The repartition of the blocks was defined in order both to have around 12 t per slab and a repartition close to 2.2 t.m^{-2} .

2.4. CEA Saclay shaking table

Seismic tests are performed on the 6 degrees of freedom AZALEE shaking table at the Seismic Mechanic Study Laboratory of CEA Saclay (France). The shaking table is a 6 x 6 m aluminium square plate with a maximum payload of 100 tons (see Figure 3). The upper plate is equipped with 144 anchoring points. Eight hydraulic actuators (4 horizontal excitations and 4 vertical) are connected to the plate. The distance between two vertical actuators is 4 meters. The distance between 2 horizontal actuators is 7.06 m. The axes of horizontal actuators are located at 0.52 m below the upper face of the

shaking table. Each actuator can provide a maximum force of 1000 kN. Four static pneumatic supports under the plate uphold the weight of the table and the mock-up. The maximum displacement amplitude range is 250 mm for the two horizontal axes and 200 mm for the vertical axis.

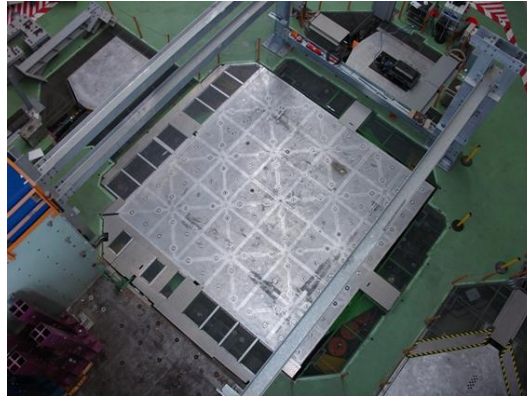


Figure 3. Picture of AZALEE shaking table (CEA Saclay, France)

2.5. Seismic inputs

Bi-axial horizontal seismic accelerations are applied to the mock-up. The tests sequence was realised as follows in two steps. First, two seismic tests with 2 different sets of real accelerograms, at 0.05 g PGA level. The sets of two real accelerograms were selected in order to slightly damage the mock-up artificially. In order to respect the scaling factor of the mock-up, the time of the accelerograms has been divided by two. The real accelerograms have been scaled by a factor between 1.03 and 1.58 in order to have a PGA level close to 0.05g (minimum level required for the tests). Second, eleven seismic tests with the set of synthetic accelerograms, scaled from 0.1 g up to 1.0 g PGA level. The set of synthetics accelerograms has been derived from the design response spectra. The PGA levels corresponding to each experimental run are presented in Table 4.

Table 4. Maximum PGA levels for the main runs

Run number	3	4	5	6	7	8	9	10	11	12	15	18	21
Max. PGA X (g)	0.08	0.08	0.19	0.21	0.19	0.23	0.33	0.41	0.41	0.54	0.58	0.70	0.75
Max. PGA Y (g)	0.03	0.05	0.15	0.24	0.21	0.32	0.35	0.55	0.56	0.67	0.77	1.06	1.13

3. NUMERICAL ANALYSIS

3.1. Finite element mesh

In order to save computational time, the finite element model has been built using finite element with a reduced kinematic. Plates have been used to describe the geometry of the shear walls, of the plates and of the reinforced concrete beams with eccentricities (central beams). Multifiber beam element has been used to model the column. The foundation has been described by mean of solid finite elements in order to ensure the kinematic compatibility of the mock-up model with the shaking table model. An overview of the overall finite element model is shown in Figure 4. Especially, one can observe that the shaking table has been considered as a constitutive part of the model. Indeed, the experience has witnessed that boundary condition conditions between the shaking table and the mock-up as well as local strains could be considered as an important contributing factor to the modal response of the structural system. Therefore, one has decided for this study to make the finite element model accounting for mock-up/shaking table interaction.

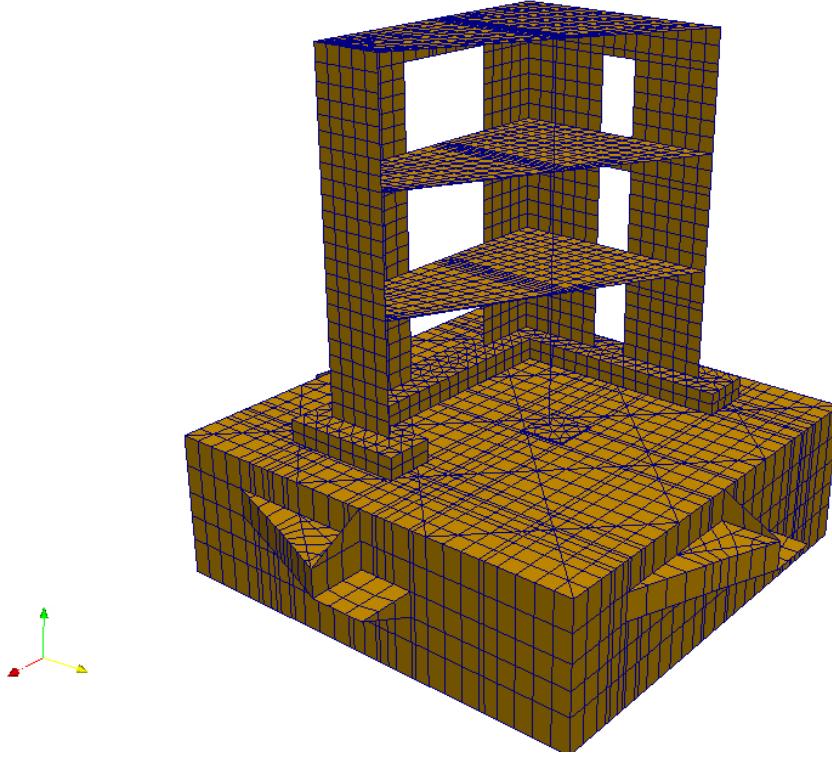


Figure 4. Finite element mesh used to mode SMART 2008 mock-up considering the shaking table interaction.

3.2. Efficient constitutive models for concrete

3.2.1. General concepts

The constitutive materials of the shaking table model have been identified according to previous work done in CEA (Le Maout *et al*, 2010), therefore one has decided not to detail this component of the model. The proposed constitutive law has been designed within the theoretical framework of the irreversible processes thermodynamic (Lemaitre *et al*, 2004) what ensures that physic principles are fulfilled. More precisely, it is based on isotropic continuum damage theory. The main idea of the constitutive law is to model in a refined way the degradation in tension and in a coarser way in compression. Indeed, since cracking is mainly responsible for the dissipation, it seems essential to pay a specific attention to that part of the behaviour. On the contrary, it is fairly rare that concrete fails in compression and therefore, this part of the behaviour can be model coarser. To ensure a numerical efficiency at the structural level, a scalar damage variable is considered to model tension. Furthermore, concrete exhibits hysteretic loops that can be explained by the activation of nonlinear frictional mechanisms between the crack lips. Taking into account such mechanisms is of primary importance when dealing with seismic analysis to obtain satisfactory responses when loading/unloading. Damage and internal sliding have been modelled in a coupled way according to the original approach proposed by (Ragueneau, 1999) for 1D cases and by (Richard *et al*, 2010) for 3D cases. In the compression if modelled by well-known non-associative plasticity that allows accounting for dilatancy and hydrostatic pressure sensitivity. One can notice that permanent strain in tension and in compression should therefore be taken into account. Last, the unilateral phenomenon that appears when cracks open and close is also considered since the proposed model is designed for cyclic (seismic) applications.

3.2.2. Thermodynamic state potential

The thermodynamic state potential can be expressed as:

$$\rho\psi = \frac{1}{2} \left(\varepsilon_{ij} - \delta d\varepsilon_{ij}^{\pi} - \varepsilon_{ij}^p \right) C_{ijkl} \left(\varepsilon_{kl} - \delta d\varepsilon_{kl}^{\pi} - \varepsilon_{kl}^p \right) + \frac{\gamma}{2} \alpha_{ij} \alpha_{ij} + H(z) + R(p) \quad (1)$$

where ρ is the material density, ε_{ij} is the total strain tensor, δ is the closure variable, d is the isotropic damage variable, ε_{kl}^π is the internal sliding tensor, ε_{ij}^p is the plastic strain tensor, α_{ij} is the kinematic hardening tensor, z is the isotropic hardening variable, p is the cumulative plastic strain, H is the consolidation function related to damage, R is the consolidation function related to the plastic strain that is activated in compression, C_{ijkl} is the elastic Hooke's tensor and γ is a kinematic hardening modulus. One can point out the fact that the proposed thermo dynamical state potential exhibits the mathematical requirements such as convexity and differentiability.

3.2.3. State equations

The state equations can be obtained from the state potential by differentiating it with respect to each state variable. The first state law linking the total strain tensor with the Cauchy stress tensor σ_{ij} is:

$$\sigma_{ij} = \frac{\partial \rho \psi}{\partial \varepsilon_{ij}} = -\frac{\partial \rho \psi}{\partial \varepsilon_{ij}^p} = C_{ijkl}(\varepsilon_{kl} - \delta d \varepsilon_{kl}^\pi - \varepsilon_{kl}^p) \quad (2)$$

Assuming the stress state is mainly in tensile, one has $\varepsilon_{ij}^p = 0_{ij}$. Furthermore, when unloading the closure variable δ is varying from 1 to 0 in a continuous way. As soon as it reaches the value 0, the linear elastic relation is clearly recovered. The sliding stress σ_{ij}^π is expressed as follows:

$$\sigma_{ij}^\pi = -\frac{\partial \rho \psi}{\partial \varepsilon_{ij}^\pi} = d C_{ijkl}(\varepsilon_{kl} - \delta \varepsilon_{kl}^\pi) \quad (3)$$

The back stress X_{ij} is expressed as:

$$X_{ij} = \frac{\partial \rho \psi}{\partial \alpha_{ij}} = \gamma \alpha_{ij} \quad (4)$$

Due to the asymmetric nature of concrete in tension/compression, the management of this type of behaviour requires defining two distinct hardenings: a first one that is activated in tension (related to damage) and a second that is activated in compression (related to plasticity). The thermodynamic force related to isotropic hardening in tension is:

$$Z = \frac{\partial \rho \psi}{\partial z} = \frac{dH(z)}{dz} \quad (5)$$

The thermodynamic force related to plasticity is:

$$R = \frac{\partial \rho \psi}{\partial p} = \frac{\partial R(p)}{\partial p} \quad (6)$$

Last, one can define the dual variable related to the closure variable that has the dimension of an energy rate:

$$\theta = \frac{\partial \rho \psi}{\partial \delta} = d \varepsilon_{ij}^\pi C_{ijkl}(\varepsilon_{kl} - d \varepsilon_{kl}^\pi - \varepsilon_{kl}^p) \quad (7)$$

3.2.4. Complementary equations

The flow rules are defined in order to manage the dissipative mechanisms taken into account by the constitutive law. A flow coupling is considered in order to manage the both isotropic damage and the corresponding isotropic hardening. The damage threshold surface f_d is expressed as:

$$f_d = \bar{Y} - (Y_0 + Z) > 0 \quad (8)$$

where \bar{Y} is the energy rate, Y_0 is an initial threshold and Z the thermodynamic force related to damage defined by equation (5). The flow rules can be deduced from the well-known normality rule:

$$\dot{d} = \dot{\omega} \frac{\partial f_d}{\partial \bar{Y}} = \dot{\omega} \quad (9)$$

$$\dot{z} = -\dot{\omega} \frac{\partial f_d}{\partial Z} = -\dot{\omega} \quad (10)$$

where $\dot{\omega}$ is the Lagrange multiplier related to damage that can be computed from the consistency condition. The internal sliding mechanism is managed in a non-associative way in order to describe the nonlinearity related to hysteretic effects. The threshold function is expressed as:

$$f_\pi = \sqrt{(\sigma_{ij}^\pi - X_{ij})(\sigma_{ij}^\pi - X_{ij})} H(\sigma_{kk}) > 0 \quad (11)$$

where H is the Heaviside function of Cauchy stress tensor. This feature allows activating the internal sliding only $\sigma_{kk} > 0$ meaning the stress state is globally in tension. The pseudo-potential of dissipation is:

$$\varphi_\pi = \sqrt{(\sigma_{ij}^\pi - X_{ij})(\sigma_{ij}^\pi - X_{ij})} + \frac{a}{2} X_{ij} X_{ij} \quad (12)$$

where a is a material parameters managing the frictional sliding that needs to be identified. The flow rules are deduced as previously using the normality rules with respect to the pseudo-potential of dissipation φ_π . The plasticity mechanism in compression is managed by mean of a non-associative flow rules based on Drucker-Prager threshold surface. This mechanism is activated only when $\sigma_{kk} < 0$ meaning that the stress state is globally in compression. More details about the theoretical formulation can be found in (Richard *et al*, 2012).

3.2.5. Local results

The stress/strain curve is shown in Figure 5. One can observe that the proposed concrete constitutive law accounts for asymmetry in tension/compression, nonlinear hysteretic effects in tension, permanent strains not only in tension but also in compression and a linear full unilateral effect.

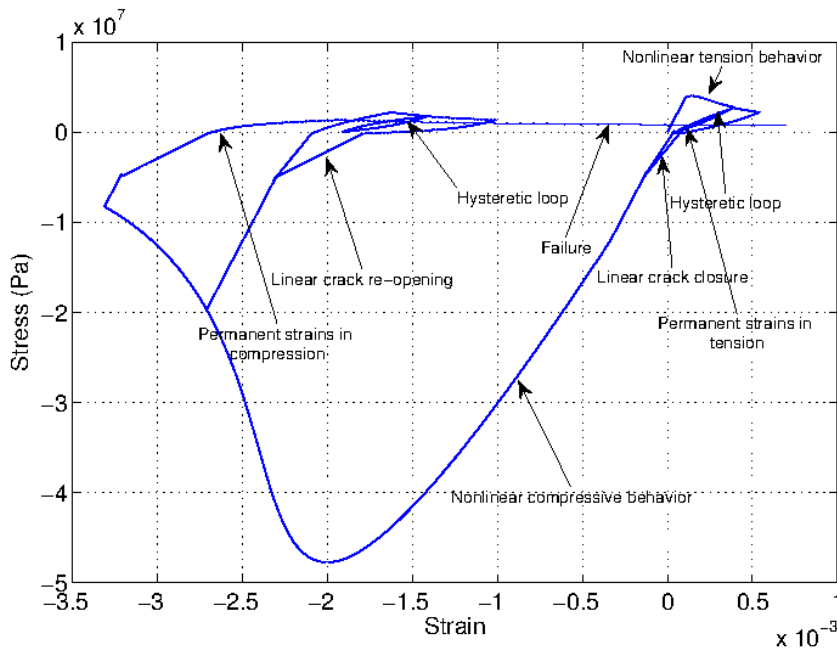


Figure 5. Stress/strain relation for concrete.

3.3. Boundary conditions

The computations are carried out in the relative axis system, meaning that the contact points of the height actuators are fixed. The mock-up is connected to the shaking table model by prescribing kinematic constraints that lie in ensuring that the distance between the contact nodes between the top plate of the shaking table and the mock-up remain constant along the time. Corresponding forces are computed to fulfil these conditions.

3.4. Input ground motion

The accelerograms measured at the mass centre of the shaking table are converted into a force field (multiplication of the mass matrix by the acceleration vector) that is applied on the whole structure. One can notice that the underlying hypothesis lies in considering the shaking table as a rigid body. This seems justified in itself considering that the boundary conditions are those that are applied to the contact points of the actuators. The input ground motion is depicted in terms of acceleration versus time in Figure 6. One can observe that the PGA is close to 0.2 g in both directions. This value is commonly considered as the reference in design codes.

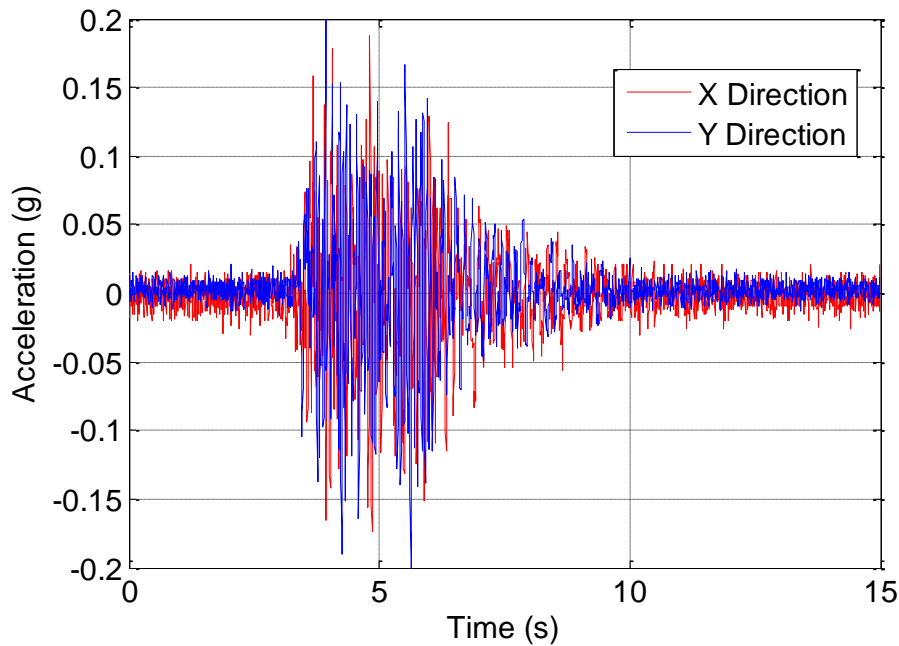


Figure 6. Input ground motion in X and Y directions.

4. RESULTS AND DISCUSSION

This section aims at presenting some numerical results compared to the experimental ones at the structural level. The computations have been performed with the opened sources finite element software Cast3M-CEA (Cast3M-CEA).

4.1. Damage pattern

Thanks to the use of the proposed constitutive model for describing the mechanical behaviour of concrete, it is possible to observe qualitatively the damage pattern over the reinforced concrete mock-up. It is presented in Figure 7. One can observe that the shear wall #4 the most damaged area. This has been experimentally observed (Chaudat *et al*, 2010). Furthermore, as expected, the areas located close to the openings are subjected to cracking.

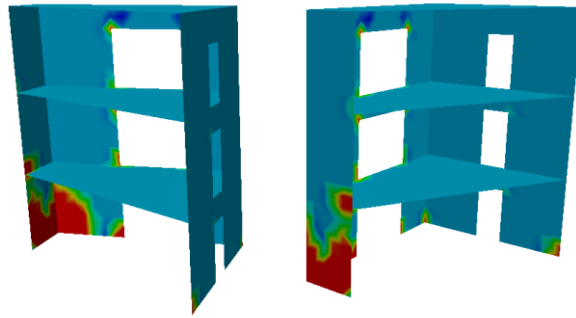


Figure 7. Damage pattern after RUN5.

4.2. Displacement time history

Due to the high amount of data recorded during the experiment, one is focused only on the point D located at the third floor (see Figure 1). The results are expressed in terms of relative displacement versus time according to the X direction. The results are shown in Figure 8. A fairly good agreement with the experience can be observed.

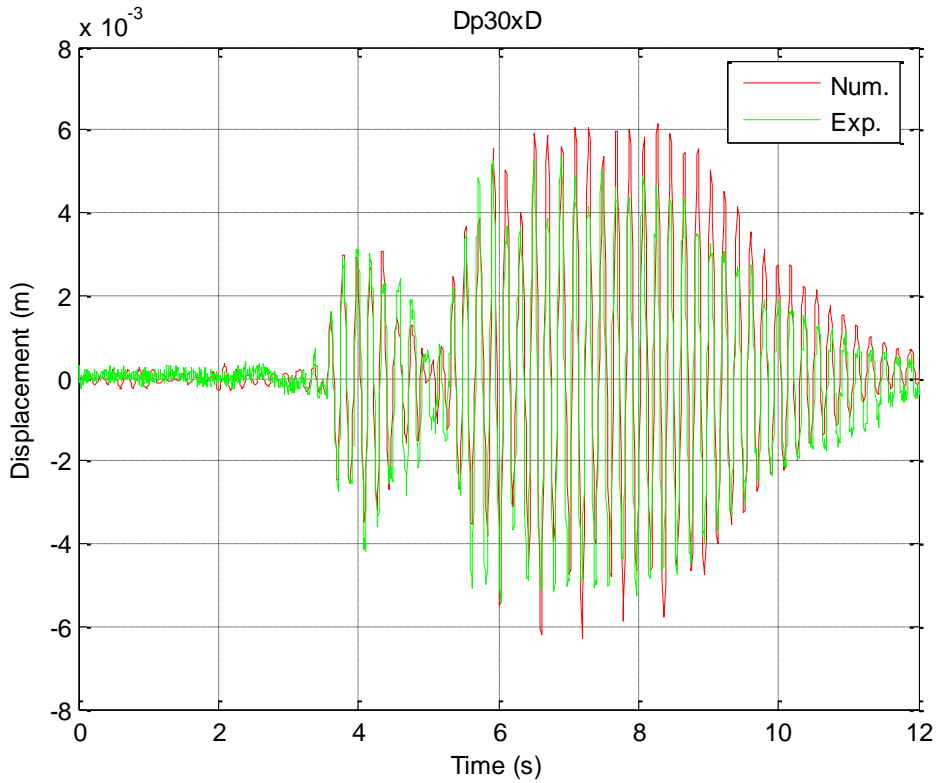


Figure 8. Displacement versus time at point D – 3rd floor – X Direction.

4.3. Acceleration time history

The acceleration versus time computed at the same point as the one previously mentioned is compared to the experimental measurements. The comparison is depicted in Figure 9. A satisfactory agreement can be observed, showing that the structural model is fully capable (at least at the design level) representing the behaviour of the system composed of the mock-up and of the shaking table.

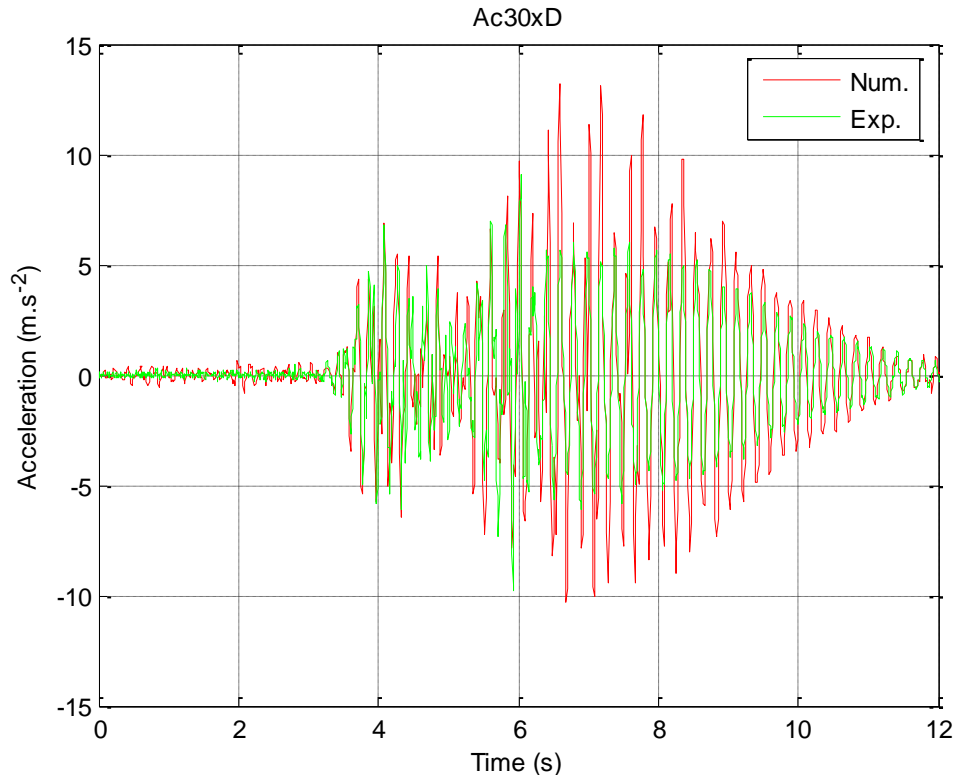


Figure 9. Acceleration versus time at point D – 3rd floor – X Direction.

5. CONCLUSION AND OUTLOOKS

In this paper, an application of a new concrete constitutive law has been presented. The structural case of the SMART 2008 mock-up that has been tested in the shaking table AZALEE-CEA has been considered. The main constitutive equations have been exposed as well as the finite element model. Some numerical results have been compared to the experimental ones and a satisfactory agreement is pointed out. One can notice that such a good agreement could not have been reached if the shaking table had not been modelled.

REFERENCES

- Cast3M-CEA. <http://www-cast3m.cea.fr>.
- Chaudat T., Juster-Lermitte S., Garnier C., Vasic S., Poupin S., Le Corre M., Mahe M. (2010). SMART 2008 Test Report. *CEA Internal Report* 10-007/B.
- Le Maoult A., Queval JC., Bairrao R. (2010). Dynamic interaction between the shaking table and the specimen during the seismic tests. *Advances in Performance-Based Earthquake Engineering*: 13, 431-440.
- Lemaître J, Chaboche JL.(2004). *Solid material mechanics*, Dunod.
- Ragueneau F. (1999). Dynamical study of concrete structures – influence of hysteretical effects. PhD thesis, Ecole Normale Supérieure de Cachan, Cachan, France.
- Richard B., Ragueneau F., Delaplace A., Oliver C. (2012). Continuum damage mechanics based model for quasi-brittle materials subjected to cyclic loadings: application to concrete. *International Conference on Strategies for Sustainable Concrete Structures*. Proceedings to be published.
- Richard B., Ragueneau F., Cremona C., Adelaide L. (2010). Isotropic continuum damage mechanics for concrete under cyclic loading: stiffness recovery, inelastic strains and frictional sliding. *Engineering Fracture Mechanics*: 77, 1203-1223.